

Critical Spin Fluctuation Mechanism for the Spin Hall Effect

Satoshi Okamoto,^{1,*} Takeshi Egami,^{1,2,3} and Naoto Nagaosa^{4,5}

¹*Materials Science and Technology Division, Oak Ridge National Laboratory, Oak Ridge, Tennessee 37831, USA*

²*Department of Materials Science and Engineering,*

The University of Tennessee, Knoxville, Tennessee 37996, USA

³*Department of Physics and Astronomy, The University of Tennessee, Knoxville, Tennessee 37996, USA*

⁴*Department of Applied Physics, The University of Tokyo, Bunkyo-ku, Tokyo 113-8656, Japan*

⁵*RIKEN Center for Emergent Matter Science (CEMS), Wako, Saitama 351-0198, Japan*

We propose mechanisms for the spin Hall effect in metallic systems arising from the coupling between conduction electrons and local magnetic moments that are dynamically fluctuating. Both a side-jump-type mechanism and a skew-scattering-type mechanism are considered. In either case, dynamical spin fluctuation gives rise to a nontrivial temperature dependence in the spin Hall conductivity. This leads to the enhancement in the spin Hall conductivity at nonzero temperatures near the ferromagnetic instability. The proposed mechanisms could be observed in 4d or 5d metallic compounds.

Introduction.—The spin Hall (SH) effect is the generation of spin current along the transverse direction by an applied electric field [1, 2]. Because it allows us to manipulate magnetic quanta, i.e., spins, without applying a magnetic field, this would become a key component in creating efficient spintronic devices. By combining the SH effect and its reciprocal effect, the inverse SH effect [3], a variety of phenomena have been demonstrated (for recent review, see Refs. [4, 5]). As in the anomalous Hall effect [6], the relativistic spin-orbit coupling (SOC) plays the fundamental role for the SH effect, and both intrinsic mechanisms [7, 8] and extrinsic mechanisms [9–12] have been proposed. Whereas many theoretical studies considered static disorder or impurities at zero temperature, the effect of nonzero temperature T in the SH effect has been addressed using phenomenological electron-phonon coupling [13, 14] or first-principle scattering approach [15].

At present, the intensity of the SH effect is too weak for practical applications [16]. One of the pathways to enhance the spin-charge conversion efficiency or the SH angle $\Theta_{SH} = \sigma_{SH}/\sigma_c$, where $\sigma_{SH(c)}$ corresponds to the SH (charge) conductivity, is to reduce the charge conductivity σ_c . For example, Ref. [17] proposed to use 5d transition-metal oxides, IrO_2 , where the strong SOC comes from Ir, rather than metallic materials. The SH effect in the surface state of topological insulators with spin-momentum locking has been also studied [18]. More recently, Jiao *et al.* reported the significant enhancement in SH effect in metallic glasses at finite temperatures [19]. Because such enhancement is not expected in crystalline systems [20], it was suggested that local structural fluctuations [13, 21] are responsible for this effect, similar to the phonon skew-scattering mechanism. Thus, the fluctuations of lattice or some other degrees of freedom at finite temperatures could provide a route to improve the efficiency of the SH effect.

For magnetic systems, the effect of finite tempera-

tures has been studied for the anomalous Hall effect in terms of skew scattering [22] and resonant skew scattering [23–25]. Theories for the resonant skew scattering were further developed by considering strong quantum spin fluctuations for systems with the time-reversal symmetry (TRS), therefore for the SH effect rather than the anomalous Hall effect [26–28]. Later, the relation between the anomalous Hall effect below the ferromagnetic transition temperature T_C and the SH effect above T_C was investigated by including nonlocal magnetic correlations in Kondo’s model [29, 30]. A recent investigation on $\text{Fe}_x\text{Pt}_{1-x}$ alloys also reported the enhancement in the SH effect near T_C [31]. So far, the magnetic fluctuation at finite temperatures has been theoretically treated on a single-site level [26–28] or using static approximations [22–25, 29]. When localized moments have long-range dynamical correlations near a magnetic instability, it is required to go beyond such a treatment (for example, see Refs. [32–35]). This could open new pathways for novel spintronics.

In this paper, we address the effect of such magnetic fluctuations onto the SH effect by calculating the SH conductivity of a model system in which conduction electrons are interacting with dynamically fluctuating local magnetic moments. We start from defining our model Hamiltonian and then identify two different mechanisms for the SH effect. The similarity and dissimilarity with the SH effect arising from impurity potential scattering or phonon scattering are discussed. The SH conductivity is computed using the Matsubara formalism by combining the self-consistent renormalization theory [34]. We show that the SH conductivity is enhanced at low temperatures when the system is in close vicinity to the ferromagnetic critical point at $T = 0$. Possible realization of this effect in 4d or 5d metallic compounds is discussed.

Model and formalism.—To be specific, we consider the s - d or s - f Hamiltonian proposed by Kondo [22, 36], $H =$

*okapon@ornl.gov

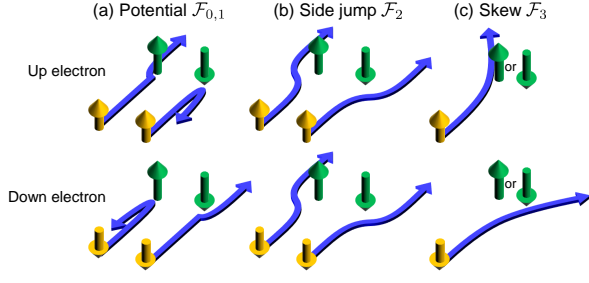


FIG. 1: Scattering processes involving (a) $\mathcal{F}_{0,1}$ terms, (b) \mathcal{F}_2 terms, and (c) \mathcal{F}_3 terms. Yellow arrows indicate conduction electrons, and green arrows indicate local moments. In the $\mathcal{F}_{2(3)}$ scattering processes, the electron deflection depends on the direction of the local moment (the electron spin), leading to the side-jump-type (skew-scattering-type) contribution to σ_{SH} .

$H_0 + H_K$ with $H_0 = \sum_{\mathbf{k}, \nu} \varepsilon_{\mathbf{k}} a_{\mathbf{k}\nu}^\dagger a_{\mathbf{k}\nu}$ and

$$H_K = -\frac{1}{N} \sum_n \sum_{\mathbf{k}, \mathbf{k}'} \sum_{\nu, \nu'} e^{i(\mathbf{k}' - \mathbf{k}) \cdot \mathbf{R}_n} a_{\mathbf{k}\nu}^\dagger a_{\mathbf{k}'\nu'} \times \left[2(\mathbf{J}_n \cdot \mathbf{s}_{\nu\nu'}) \{ \mathcal{F}_0 + 2\mathcal{F}_1(\mathbf{k} \cdot \mathbf{k}') \} + i\mathcal{F}_2 \mathbf{J}_n \cdot (\mathbf{k}' \times \mathbf{k}) + i\mathcal{F}_3 \{ (\mathbf{J}_n \cdot \mathbf{s}_{\nu\nu'}) (\mathbf{J}_n \cdot (\mathbf{k}' \times \mathbf{k})) + (\mathbf{J}_n \cdot (\mathbf{k}' \times \mathbf{k})) (\mathbf{J}_n \cdot \mathbf{s}_{\nu\nu'}) - \frac{2}{3} (\mathbf{J}_n \cdot \mathbf{J}_n) (\mathbf{s}_{\nu\nu'} \cdot (\mathbf{k}' \times \mathbf{k})) \} \right]. \quad (1)$$

Here, $a_{\mathbf{k}\nu}^{(\dagger)}$ is the annihilation (creation) operator of a conduction electron with momentum \mathbf{k} and spin ν , $\varepsilon_{\mathbf{k}} = \frac{\hbar^2 \mathbf{k}^2}{2m} - \mu$ is the dispersion relation measured from the Fermi level μ with the carrier effective mass m , $\mathbf{s}_{\nu\nu'} = \frac{1}{2} \boldsymbol{\sigma}_{\nu\nu'}$ is the conduction electron spin with $\boldsymbol{\sigma}$ the Pauli matrices, and $N(N_m)$ is the total number of lattice sites (local moments). \mathbf{J}_n is the local spin moment at position \mathbf{R}_n , when the SOC is weaker than the crystal field splitting and could be treated as a perturbation, or the local total angular momentum, when the SOC is strong so that the total angular momentum is a constant of motion. Parameters \mathcal{F}_l are related to F_l defined in Ref. [22] as discussed in the Supplemental Material [36]. In this work, we focus on three-dimensional systems. While the current analysis could be applied to other dimensions, lower-dimensional systems require more careful treatments.

In Eq. (1), $\mathcal{F}_{0,1}$ terms correspond to the standard s - d or s - f exchange interaction, acting as the spin-dependent potential scattering as schematically shown in Fig. 1 (a). $\mathcal{F}_{2,3}$ terms represent the exchange of angular momentum between a conduction electron and a local moment. These terms are odd (linear or cubic) order in J_n and s and induce the electron deflection depending on the direction of \mathbf{J}_n or \mathbf{s} as depicted in Figs. 1 (b) and ref-fig:scatter (c). As discussed below, the \mathcal{F}_2 term and the \mathcal{F}_3 term, respectively, generate the side-jump- and the

skew-scattering-type contributions to the SH conductivity.

In order to see the different types of contributions, we analyze the velocity operator, from which the charge current and the spin current operators are defined. Importantly, a side-jump-type contribution to the SH effect arises from the anomalous velocity as in the conventional SH effect. The velocity operator is defined by $\mathbf{v} = (i/\hbar)[H, \mathbf{r}]$. Among various terms, lowest order contributions to the spin Hall conductivity come from

$$\mathbf{v} = \sum_{\mathbf{k}} \frac{\hbar \mathbf{k}}{m} a_{\mathbf{k}\nu}^\dagger a_{\mathbf{k}\nu} - \frac{i}{\hbar N} \sum_n \sum_{\mathbf{k}, \mathbf{k}'} \sum_{\nu, \nu'} e^{i(\mathbf{k}' - \mathbf{k}) \cdot \mathbf{R}_n} \times \{ \mathcal{F}_2 \mathbf{J}_n + 2\mathcal{F}_3 (\mathbf{J}_n \cdot \mathbf{s}_{\nu\nu'}) \mathbf{J}_n \} \times (\mathbf{k}' - \mathbf{k}) a_{\mathbf{k}\nu}^\dagger a_{\mathbf{k}'\nu'}. \quad (2)$$

Here, a term involving \mathcal{F}_1 is neglected because it is proportional to $(\mathbf{k} + \mathbf{k}')$ and does not contribute to σ_{SH} at the lowest order. The second terms involving $\mathcal{F}_{2,3}$ are the anomalous velocity. The charge current and the spin current are then given by using the velocity operator as $\mathbf{j}^c = -e\mathbf{v}$ and $\mathbf{j}^s = -e\{\frac{1}{N} \sum_{\mathbf{k}} s_{\nu\nu'}^\dagger a_{\mathbf{k}\nu}^\dagger a_{\mathbf{k}\nu'}, \mathbf{v}\}$, respectively. Note that \mathbf{j}^c and \mathbf{j}^s have the same dimension.

Now, we consider the side-jump-type mechanism arising from the anomalous velocity in Eq. (2) combined with the spin-dependent potential scattering $\mathcal{F}_{0,1}$ in Eq. (1). At this moment, one could notice some analogy between the current model and the previous ones utilizing the potential scattering V_n [10–12] as $\mathcal{F}_{0,1} J_n s \leftrightarrow V_n$ and $\mathcal{F}_2 J_n \leftrightarrow \lambda^2 V_n s$, i.e., the spin s dependence is switched from the anomalous velocity to the scattering term. Therefore, the second-order processes involving $\mathcal{F}_{0,1}$ and \mathcal{F}_2 terms could generate the side-jump-type contribution to the SH effect. The diagrammatic representation of this side-jump-type contribution to the SH conductivity is presented in Fig. 2. Note that this contribution is $\mathcal{O}(\mathcal{F}_{0,1} \mathcal{F}_2 \langle J_n J_{n'} \rangle)$. If the \mathcal{F}_3 term in the anomalous velocity is used, it would become $\mathcal{O}(\mathcal{F}_{0,1} \mathcal{F}_3 \langle J_n J_{n'} J_{n''}^2 \rangle)$, odd order in the local moment. Such a contribution vanishes when the local moments have the TRS in a paramagnetic phase above magnetic transition temperature.

How about the skew-scattering-type contribution? Unlike the side-jump-type contribution, the \mathcal{F}_2 does not contribute to σ_{SH} arising from the third-order perturbation processes combined with $\mathcal{F}_{0,1}$ terms. This is because such processes are $\mathcal{O}(\mathcal{F}_{0,1}^2 \mathcal{F}_2 \langle J_n J_{n'} J_{n''} \rangle)$ and vanish by the TRS in the local moments. In fact, the skew-scattering-type contribution arises from the third-order processes involving $\mathcal{F}_{0,1}$ and \mathcal{F}_3 terms as $\mathcal{O}(\mathcal{F}_{0,1}^2 \mathcal{F}_3 \langle J_n J_{n'} J_{n''}^2 \rangle)$. Therefore, such skew-scattering-type contributions are possible without introducing unharmonic (third-order) magnetic correlations, while it is second order in the spin fluctuation propagator $\mathcal{O}(D^2)$ as discussed below. This contrasts with the phonon skew scattering, where unharmonic phonon interactions are essential [13].

Matsubara formalism and spin fluctuation.—In what follows, we use the Matsubara formalism to compute the

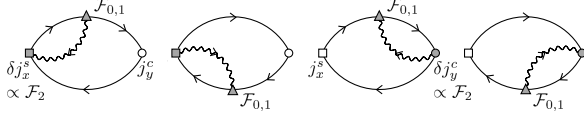


FIG. 2: Diagrammatic representation for the side-jump contribution. Solid (wavy) lines are the electron Green's functions (the spin fluctuation propagators). Squares (circles) are the spin (charge) current vertices, with filled symbols representing the velocity correction with \mathcal{F}_2 , i.e., side jump. Filled triangles are the interaction vertices with $\mathcal{F}_{0,1}$.

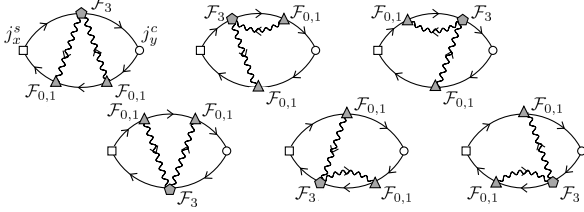


FIG. 3: Diagrammatic representation for the skew-scattering contribution. Filled pentagons are the interaction vertices with \mathcal{F}_3 . The definitions of the other symbols or lines are the same as in Fig. 2.

SH conductivity given by

$$\sigma_{SH}(i\Omega_l) = \frac{i}{i\Omega_l V} \int_0^{1/T} d\tau e^{i\Omega_l \tau} \langle T_\tau j_x^s(\tau) j_y^c(0) \rangle, \quad (3)$$

where Ω_l is the bosonic Matsubara frequency, and V is the volume of the system. At the end of the analysis, $i\Omega_l$ is analytically continued to real frequency as $i\Omega_l \rightarrow \Omega + i0^+$. We will then consider the dc limit, $\Omega \rightarrow 0$, to obtain σ_{SH} .

This formalism allows one to treat conduction electrons coupled with dynamically fluctuating local moments \mathbf{J}_n . To describe the latter, we consider a generic Gaussian action given by $A_{Gauss} = \frac{1}{2} \sum_{\mathbf{q}, l} D_{\mathbf{q}}^{-1}(i\omega_l) J_{\mathbf{q}}(i\omega_l) J_{-\mathbf{q}}(-i\omega_l)$ with $D_{\mathbf{q}}^{-1}(i\omega_l) = \delta + Aq^2 + |\omega_l|/\Gamma_q$. Here, $\omega_l = 2l\pi T$ is the bosonic Matsubara frequency, and A is introduced as a constant so that Aq^2 has the unit of energy. δ is the distance from a ferromagnetically ordered state and is related to the magnetic correlation length as $\xi^2 \propto \delta^{-1}$. $J_{\mathbf{q}}(i\omega_l)$ is a space and imaginary-time τ Fourier transform of $J_n(\tau)$, where we made the τ dependence explicit. In principle, δ depends on temperature and is determined by solving self-consistent equations for a full model including non-Gaussian terms [32–35, 37]. Γ_q represents the momentum-dependent damping. In clean metals close to the ferromagnetic instability, $\Gamma_q = \Gamma_q$. When elastic scattering exists due to impurities or disorders, q has a small cutoff $q_c \sim \ell^{-1} = 1/v_F \tau_c$ with ℓ being the mean free path of conduction electrons, $v_F = \hbar k_F/m$ the Fermi velocity, and τ_c the carrier lifetime. Therefore, the damping term at $q \lesssim q_c$ has to be replaced

by Γ_{q_c} [38]. With this propagator D , the spatial and temporal correlation of \mathbf{J}_n is given by $\langle T_\tau J_n(\tau) J_{n'}(0) \rangle = \frac{T}{N} \sum_{\mathbf{q}, l} e^{-i\omega_l \tau + i\mathbf{q} \cdot (\mathbf{R}_n - \mathbf{R}_{n'})} D_{\mathbf{q}}(i\omega_l)$. Theoretical analyses based on this model have been successful to explain many experimental results on itinerant magnets [34].

Because of the phase factor $e^{i\mathbf{q} \cdot (\mathbf{R}_n - \mathbf{R}_{n'})}$, the ferromagnetic fluctuation is essential for the SH effect. When the spin fluctuation has characteristic momentum $\mathbf{Q} \neq 0$, $e^{i\mathbf{Q} \cdot (\mathbf{R}_n - \mathbf{R}_{n'})}$ has destructive effects.

Spin-Hall conductivity.—With the above preparations, now we proceed to examine the SH conductivity. Based on the diagrammatic representations in Figs. 2 and 3, σ_{SH} is expressed in terms of electron Green's function G and the propagator of local magnetic moments D . The full expression is presented in Ref. [36].

We carry out the Matsubara summations, the energy integrals and the momentum summations as detailed in Ref. [36] to find

$$\sigma_{SH}^{side\ jump} \approx \frac{2e^2 n_m^2}{m} \tau_c I(T, \delta) \left(\frac{1}{3} \mathcal{F}_0 k_F^2 - \frac{2}{5} \mathcal{F}_1 k_F^4 \right) \mathcal{F}_2 N_F \quad (4)$$

for the side-jump contribution and

$$\sigma_{SH}^{skew\ scat.} \approx \frac{4e^2 \hbar n_m^3}{m^2} \tau_c^2 I^2(T, \delta) \left(\mathcal{F}_0 + \mathcal{F}_1 k_F^2 \right)^2 \mathcal{F}_3 \frac{2k_F^4}{15} N_F \quad (5)$$

for the skew-scattering contribution. Here, $n_m = N_m/N$ is the concentration of local moments, and $N_F = mk_F/2\pi^2 \hbar^2$ is the electron density of states per spin at the Fermi level. The function $I(T, \delta)$ defined in Ref. [36] is the direct consequence of the coupling between conduction electrons and the dynamical spin fluctuation. There are a number of limiting cases where the analytic form of $I(T, \delta)$ is available. For clean systems ($\Gamma_q = \Gamma_q$, i.e., no momentum cutoff) at low temperatures, where $\delta + A(aT/\hbar v_F)^2 \ll \hbar v_F/\Gamma$ is satisfied, $I(T, \delta) \approx \frac{1}{8\pi\delta} (aT/\hbar v_F)^3$ with a being the lattice constant. When the system is on the quantum critical point for the ferromagnetic ordering, δ is scaled as $\delta \propto T^{4/3}$ [34]. Thus, $I(T, \delta) \propto T^{5/3}$ is expected. For clean systems at high temperatures, where $\delta + A(aT/\hbar v_F)^2 \gg \hbar v_F/\Gamma$ is satisfied, $I(T, \delta) \approx \frac{\hbar v_F}{4\pi^2 \Gamma \delta^2} (aT/\hbar v_F)^3$. At such high temperatures, δ is linearly dependent on T [34, 39]. Therefore, one expects $I(T, \delta) \propto T$. Similar analyses are possible for dirty systems, where Γ_q has a small momentum cutoff. In this case, one expects $I(T, \delta) \propto T$ at both low temperatures and high temperatures (see Ref. [36] for details).

In addition to $I(T, \delta)$, the temperature dependence of σ_{SH} is induced by the carrier lifetime τ_c . This quantity comes from several different contributions as

$$\tau_c^{-1} = \tau_{sf}^{-1} + \tau_{ee}^{-1} + \tau_{ep}^{-1} + \tau_{dis}^{-1} + \dots \quad (6)$$

Here, τ_{sf}^{-1} is from the scattering due to the spin fluctuation. Using H_K and the same level of approximation, τ_{sf}^{-1} is given by $\tau_{sf}^{-1} \approx \frac{2n_m^2}{\hbar} I(T, \delta) (\mathcal{F}_0 + 2\mathcal{F}_1 k_F^2)^2$ [36]. τ_{sf}^{-1} and $I(T, \delta)$ have the same T dependence as schematically

shown in Fig. 4 (a). τ_{ee}^{-1} and τ_{ep}^{-1} are from the electron-electron interactions and the electron-phonon interactions, respectively. Their leading T dependence is given by $\tau_{ee}^{-1} \approx \tau_{ee,0}^{-1}(T/T_F)^2$ [40] and $\tau_{ep}^{-1} \approx \tau_{ep,0}^{-1}(T/T_D)^5$ [41, 42], where $T_{F(D)}$ is the Fermi (Debye) temperature. τ_{dis}^{-1} is from the disorder effects, and its T dependence is expected to be small. Figure 4 (b) summarizes the T dependence of $\tau_{dis,ee,ep}^{-1}$.

The overall T dependence of σ_{SH} is determined by the combination of $I(T, \delta)$ and τ_c . The strong enhancement is thus expected at the ferromagnetic critical point, where the magnetic correlation length $\xi \propto \delta^{-1/2}$ diverges as $T^{-2/3}$. This results in τ_{sf}^{-1} and hence the electrical resistivity σ_c^{-1} scaled as $T^{5/3}$ [39]. Since $\tau_{sf}^{-1} \propto I(T, \delta)$, $\sigma_{SH}^{side\ jump}$ and $\sigma_{SH}^{skew\ scat.}$ are expected to be maximized when the spin fluctuation dominates τ_c as

$$\sigma_{SH,max}^{side\ jump} \approx \frac{e^2 \hbar}{m} \frac{\mathcal{F}_2 k_F^2}{3\mathcal{F}_0} N_F \quad (7)$$

and

$$\sigma_{SH,max}^{skew\ scat.} \approx \frac{e^2 \hbar^3}{m^2 n_m} \frac{2\mathcal{F}_3 k_F^4}{15\mathcal{F}_0^2} N_F, \quad (8)$$

respectively, at low but nonzero temperature T_{max} . This T_{max} is approximately given by $T_F(5\tau_{ee,0}/\tau_{dis})^{1/2}$ when $T_F \ll T_D$ or $T_D(\tau_{ep,0}/2\tau_{dis})^{1/5}$ when $T_F \gg T_D$. As the temperature is lowered to zero, σ_{SH} goes to zero as $\sigma_{SH}^{side\ jump} \propto \tau_{dis} I(T, \delta) \propto T^{5/3}$ and $\sigma_{SH}^{skew\ scat.} \propto \tau_{dis}^2 I^2(T, \delta) \propto T^{10/3}$ because of the nonzero τ_{dis}^{-1} , and the residual SH conductivity is due to disorders or impurities. At higher temperatures, the carrier lifetime is suppressed by the electron-electron or electron-phonon interaction, and therefore σ_{SH} is decreased. The overall T dependence of $\sigma_{SH}^{skew\ scat.}$ is schematically shown in Fig. 4 (c).

In dirty systems, Γ_q involves a small cutoff momentum. Because τ_{dis} is dominant, we expect $\sigma_{SH}^{side\ jump} \propto T$ and $\sigma_{SH}^{skew\ scat.} \propto T^2$ at low temperatures as discussed in Ref. [36]. When the temperature is increased above $T \sim \min\{T_F, T_D\}$, σ_{SH} decreases with T because τ_c is suppressed. Thus, σ_{SH} is expected to be maximized at around T_{max} as discussed for clean systems, yet the maximum value depends explicitly on τ_c 's. In fact, the enhancement in $\tau_{sf,ee,ep}^{-1}$ with increasing T always induces a momentum cutoff in the damping term Γ_q at high temperatures. Therefore, we expect that clean systems and dirty systems behave similarly at high temperatures, i.e., $\sigma_{SH}^{side\ jump} \propto \tau_c T$ and $\sigma_{SH}^{skew\ scat.} \propto \tau_c^2 T^2$.

Discussion.—How realistic is the current spin fluctuation mechanism? Here, we provide rough estimations of $\sigma_{SH,max}^{side\ jump}$ and $\sigma_{SH,max}^{skew\ scat.}$. According to a free electron model, \mathcal{F}_0 is expected to be ~ 0.1 eV for both transition metal and actinide compounds [43]. (In Ref. [43], J_0 , corresponding to \mathcal{F}_0 in this study, was estimated to be 0.7×10^{-12} erg for the s - d interaction in Mn and 2.5×10^{-13} erg for the s - f interaction in Gd.)

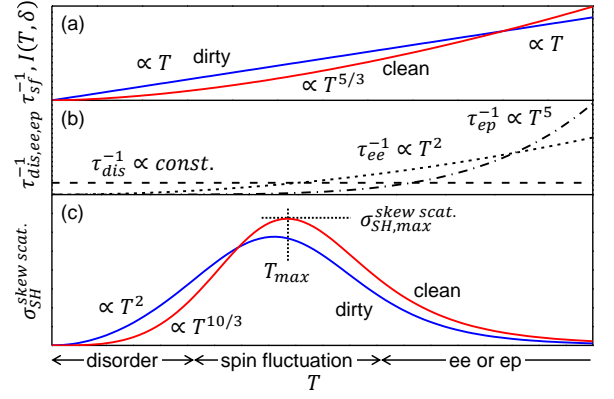


FIG. 4: Schematic temperature dependence of (a) τ_{sf}^{-1} and $I(T, \delta)$, (b) τ_{dis}^{-1} (dashed line), τ_{ee}^{-1} (dotted line), and τ_{ep}^{-1} (dash-dotted line), and (c) $\sigma_{SH}^{skew\ scat.}$. Red lines and blue lines correspond to the clean system and the dirty system, respectively. At a low (intermediate, high) temperature regime, τ_c^{-1} is dominated by τ_{dis}^{-1} (τ_{sf}^{-1} , τ_{ee}^{-1} or τ_{ep}^{-1}), creating $\sigma_{SH,max}^{skew\ scat.}$ at T_{max} .

Since $\mathcal{F}_{2,3} k_F^2$ involve the integral of higher-order spherical Bessel functions, $j_{1,3}$, i.e., p -wave scattering, than \mathcal{F}_0 , j_0 , i.e., s -wave scattering [22], $\mathcal{F}_{2(3)} k_F^2$ would be an order (two orders) of magnitude smaller than \mathcal{F}_0 . Therefore, taking a rough estimation $\mathcal{F}_2 k_F^2 \sim 0.01$ eV, $\mathcal{F}_3 k_F^2 \sim 0.001$ eV and typical values of $k_F/\pi \sim 10^9$ m $^{-1}$ and $\frac{\hbar^2 k_F^2}{2m} = \mu \sim 10$ eV [44] for s electrons in metallic compounds, optimistic estimations are $\sigma_{SH,max}^{side\ jump} \sim 10^3$ $\Omega^{-1}\text{m}^{-1}$ and $\sigma_{SH,max}^{skew\ scat.} \sim 10^5$ $\Omega^{-1}\text{m}^{-1}$. The difference in magnitude between $\sigma_{SH,max}^{side\ jump}$ and $\sigma_{SH,max}^{skew\ scat.}$ comes from the small factor $\mathcal{F}_2/\mathcal{F}_0$ in $\sigma_{SH,max}^{side\ jump}$ and the large factor μ/\mathcal{F}_0 in $\sigma_{SH,max}^{skew\ scat.}$. Thus, $\sigma_{SH,max}^{skew\ scat.}$ could be comparable to the largest σ_{SH} reported so far [16].

Could there be systems that show the SH effect by the proposed mechanisms? The crucial ingredients are the coupling between conduction electrons and localized but not ordered magnetic moments. Suitable candidate materials would be $4d$ or $5d$ metallic compounds with partially filled d shells, such as Ir, Pt, W and Re. Because of the large SOC than $3d$ compounds, the intrinsic mechanism could contribute to the SH effect. One route to enhance σ_{SH} further is doping with magnetic $3d$ transition metal elements to enhance the ferromagnetic spin fluctuation. It would be possible to distinguish between the intrinsic mechanism and the extrinsic mechanisms discussed in this work by comparing crystalline samples and disordered samples such as metallic glasses. In fact, metallic glasses might be a good choice in trying to enhance the SH angle Θ_{SH} . Since the carrier lifetime in metallic glasses is dominated by the structure factor, the temperature dependence of $\tau_c \sim \tau_{dis}$ is small [45, 46]. Using the same formalism, the longitudinal charge conductivity is given by $\sigma_c = 2e^2 \tau_c k_F^3 / 3m\pi^2$. Therefore, $\Theta_{SH} =$

σ_{SH}/σ_c is more sensitive to the spin fluctuation contribution than σ_{SH} itself. Since $\sigma_{SH}^{skew\,scat.}$ is dominant, the spin fluctuation contribution $I(T, \delta)$ could be extracted from σ_{SH}/σ_c^2 . Recently, Ou *et al.* reported very large $\Theta_{SH} > 0.34$ in $\text{Fe}_x\text{Pt}_{1-x}$ alloys near T_C [31]. While the detailed analyses remain to be carried out, with the typical conductivity in their sample $\sigma_c \sim 10^6 \, \Omega^{-1}\text{m}^{-1}$ and our theoretical $\sigma_{SH, max}^{skew\,scat.} \sim 10^5 \, \Omega^{-1}\text{m}^{-1}$, Θ_{SH} is estimated to be ~ 0.1 , that is comparable to this report.

To summarize, we investigated the effect of fluctuating magnetic moments on the spin Hall effect in metallic systems. We employed the microscopic model developed by Kondo for the coupling between conduction electrons and localized moments [22] and analyzed the fluctuation of local moments using the self-consistent renormaliza-

tion theory by Moriya [34]. As in the conventional spin Hall effect due to the impurity scattering, a side-jump-type mechanism and a skew-scattering-type mechanism appear. Because of the dynamical spin fluctuation, the spin Hall conductivity has a nontrivial temperature dependence, leading to the enhancement at nonzero temperatures near the ferromagnetic instability. The skew scattering mechanism we proposed could generate a sizable spin Hall effect.

The research by S.O. and T.E. was supported by the U.S. Department of Energy, Office of Science, Basic Energy Sciences, Materials Sciences and Engineering Division. N.N. was supported by JST CREST Grant No. JPMJCR1874 and JPMJCR16F1, Japan, and JSPS KAKENHI Grants No. 18H03676 and No. 26103006.

-
- [1] M. I. Dyakonov and V. I. Perel, JETP Lett. **13**, 467; Phys. Lett. **35A**, 459 (1971).
 - [2] J. E. Hirsch, Phys. Rev. Lett. **83**, 1834 (1999).
 - [3] E. Saitoh, M. Ueda, H. Miyajima, and G. Tatara, Appl. Phys. Lett. **88**, 182509 (2006).
 - [4] S. Murakami and N. Nagaosa, (2011) *Spin Hall Effect. Comprehensive Semiconductor Science and Technology 1* (Elsevier, New York, 2011), pp. 222-278.
 - [5] J. Sinova, S. O. Valenzuela, J. Wunderlich, C. H. Back, and T. Jungwirth, Rev. Mod. Phys. **87**, 1213 (2015).
 - [6] N. Nagaosa, J. Sinova, S. Onoda, A. H. MacDonald, and N. P. Ong, Rev. Mod. Phys. **82**, 1539 (2010).
 - [7] J. Sinova, D. Culcer, Q. Niu, N. A. Sinitsyn, T. Jungwirth, and A. H. MacDonald, Phys. Rev. Lett. **92**, 126603 (2004).
 - [8] S. Murakami, N. Nagaosa, and S.-C. Zhang, Phys. Rev. Lett. **93**, 156804 (2004).
 - [9] J. Smit, Physica (Amsterdam) **21**, 877 (1955); **24** 39 (1958).
 - [10] L. Berger, Phys. Rev. B **2**, 4559 (1970); **5**, 1862 (1972).
 - [11] A. Crépieux and P. Bruno, Phys. Rev. B **64**, 014416 (2001).
 - [12] W.-K. Tse and S. Das Sarma, Phys. Rev. Lett. **96**, 056601 (2006).
 - [13] C. Gorini, U. Eckern, and R. Raimondi, Phys. Rev. Lett. **115**, 076602 (2015).
 - [14] C. Xiao, Y. Liu, Z. Yuan, S. A. Yang, and Q. Niu, Phys. Rev. B **100**, 085425 (2019).
 - [15] L. Wang, R. J. H. Wesselink, Y. Liu, Z. Yuan, K. Xia, and P. J. Kelly, Phys. Rev. Lett. **116**, 196602 (2016).
 - [16] A. Hoffmann, IEEE Trans. Magn. **49**, 5172, (2013).
 - [17] K. Fujiwara, Y. Fukuma, J. Matsuno, H. Idzuchi, Y. Niimi, Y. Otani, and H. Takagi, Nat. Commun. **4**, 2893 (2013).
 - [18] T. T. Ong and N. Nagaosa, Phys. Rev. Lett. **121**, 066603 (2018).
 - [19] W. Jiao, D. Z. Hou, C. Chen, H. Wang, Y. Z. Zhang, Y. Tian, Z. Y. Qiu, S. Okamoto, K. Watanabe, A. Hirata, T. Egami, E. Saitoh, and M. W. Chen, arXiv:1808.10371.
 - [20] L. Vila, T. Kimura, and Y. C. Otani, Phys. Rev. Lett. **99**, 226604 (2007).
 - [21] G. V. Karnad, C. Gorini, K. Lee, T. Schulz, R. Lo Conte, A. W. J. Wells, D.-S. Han, K. Shahbazi, J.-S. Kim, T. A. Moore, H. J. M. Swagten, U. Eckern, R. Raimondi, and M. Kläui, Phys. Rev. B **97**, 100405(R) (2018).
 - [22] J. Kondo, Prog. Theor. Phys. **27**, 772 (1962).
 - [23] A. Fert and O. Jaoul, Phys. Rev. Lett. **28**, 303 (1972).
 - [24] P. Coleman, P. W. Anderson, and T. V. Ramakrishnan, Phys. Rev. Lett. **55**, 414 (1985).
 - [25] A. Fert and P. M. Levy, Phys. Rev. B **36**, 1907 (1987).
 - [26] G.-Y. Guo, S. Maekawa, and N. Nagaosa, Phys. Rev. Lett. **102**, 036401 (2009).
 - [27] B. Gu, J.-Y. Gan, N. Bulut, T. Ziman, G.-Y. Guo, N. Nagaosa, and S. Maekawa, Phys. Rev. Lett. **105**, 086401 (2010).
 - [28] B. Gu, I. Sugai, T. Ziman, G. Y. Guo, N. Nagaosa, T. Seki, K. Takanashi, and S. Maekawa, Phys. Rev. Lett. **105**, 216401 (2010).
 - [29] B. Gu, T. Ziman, and S. Maekawa, Phys. Rev. B **86**, 241303(R) (2012).
 - [30] D.H. Wei, Y. Niimi, B. Gu, T. Ziman, S. Maekawa, and Y. Otani, Nat. Commun. **3**, 1058 (2012).
 - [31] Y. Ou, D. C. Ralph, and R. A. Buhrman, Phys. Rev. Lett. **120**, 097203 (2018).
 - [32] T. Moriya and A. Kawabata, J. Phys. Soc. Jpn. **34**, 639 (1973); **35**, 669 (1973).
 - [33] J. A. Hertz, Phys. Rev. B **14**, 1165 (1976).
 - [34] T. Moriya, *Spin Fluctuations in Itinerant Electron Magnetism*, Solid-State Sciences Vol. 56 (Springer-Verlag, Berlin, 1985).
 - [35] A. J. Millis, Phys. Rev. B **48**, 7183 (1993).
 - [36] See Supplemental Material for details about the theoretical model and analytical calculations.
 - [37] N. Nagaosa, *Quantum Field Theory in Strongly Correlated Electron Systems* (Springer-Verlag, Berlin, 1999).
 - [38] P. A. Lee and N. Nagaosa, Phys. Rev. B **46**, 5621 (1992).
 - [39] K. Ueda and T. Moriya, J. Phys. Soc. Jpn. **39**, 605 (1975).
 - [40] W. G. Baber, Proc. R. Soc. A **158**, 383 (1937).
 - [41] F. Bloch, Z. Phys. **59**, 208 (1930).
 - [42] J.M. Ziman, *Electrons and Phonons: The Theory of Transport Phenomena in Solids* (Clarendon, Oxford, 1960).
 - [43] T. Kasuya, Prog. Theor. Phys. **22**, 227 (1959).
 - [44] For example, R. M. Martin, *Electronic Structure: Basic Theory and Practical Methods* (Cambridge University Press, Cambridge, England, 2004).

[45] J. M. Ziman, *Philos. Mag.* **6**, 1013 (1961).

[46] J. M. Ziman, *Adv. Phys.* **16**, 551 (1967).

Supplementary material: Critical spin fluctuation mechanism for the spin Hall effect

Satoshi Okamoto,¹ Takeshi Egami,^{1,2,3} and Naoto Nagaosa^{4,5}

¹*Materials Science and Technology Division, Oak Ridge National Laboratory, Oak Ridge, Tennessee 37831, USA*

²*Department of Materials Science and Engineering, The University of Tennessee, Knoxville, Tennessee 37996, USA*

³*Department of Physics and Astronomy, The University of Tennessee, Knoxville, Tennessee 37996, USA*

⁴*Department of Applied Physics, The University of Tokyo, Bunkyo-ku, Tokyo 113-8656, Japan*

⁵*RIKEN Center for Emergent Matter Science (CEMS), Wako, Saitama 351-0198, Japan*

S1. Relation between \mathcal{F}_l and F_l in Ref. [S1]

This section provides the relation between \mathcal{F}_l appearing in Eq. (1) and F_l defined in Ref. [S1]. To make this relation transparent, we express the original Hamiltonians derived in Ref. [S1] using a more tractable form as Eq. (1).

First, we consider a weak spin-orbit coupling (SOC) case, where the SOC strength λ is smaller than the crystal field splitting Δ and, therefore, the SOC can be treated as a perturbation. For this case, the local exchange term given in Eq. (2.33) is rewritten as

$$H_K = -\frac{1}{N} \sum_n \sum_{\mathbf{k}, \mathbf{k}'} \sum_{\nu, \nu'} e^{i(\mathbf{k}' - \mathbf{k}) \cdot \mathbf{R}_n} a_{\mathbf{k}\nu}^\dagger a_{\mathbf{k}'\nu'} \left[2(\mathbf{S}_n \cdot \mathbf{s}_{\nu\nu'}) \{F_0 + 2F_1(\boldsymbol{\kappa} \cdot \boldsymbol{\kappa}')\} + i\Lambda_1 F_2 \mathbf{S}_n \cdot (\boldsymbol{\kappa}' \times \boldsymbol{\kappa}) \right. \\ \left. + i2\Lambda_1 c_2 F_2 \left\{ (\mathbf{S}_n \cdot \mathbf{s}_{\nu\nu'}) (\mathbf{S}_n \cdot (\boldsymbol{\kappa}' \times \boldsymbol{\kappa})) + (\mathbf{S}_n \cdot (\boldsymbol{\kappa}' \times \boldsymbol{\kappa})) (\mathbf{S}_n \cdot \mathbf{s}_{\nu\nu'}) - \frac{2}{3} (\mathbf{S}_n \cdot \mathbf{S}_n) (\mathbf{s}_{\nu\nu'} \cdot (\boldsymbol{\kappa}' \times \boldsymbol{\kappa})) \right\} \right]. \quad (\text{S1})$$

Here, \mathbf{S}_n is a local spin moment at site \mathbf{R}_n , $\boldsymbol{\kappa}$ and $\boldsymbol{\kappa}'$ are the unit vectors in the directions of \mathbf{k} and \mathbf{k}' , respectively. Parameters F_l are exchange interactions between local d or f orbitals and the conduction electron as defined in Eqs. (2.15–18). Λ_1 is a dimensionless parameter roughly proportional to λ/Δ as defined in Eq. (2.34) or (2.39) in Ref. [S1]. c_2 is also a dimensionless parameter $\mathcal{O}(1/10)$ – $\mathcal{O}(1)$ depending on the electron configuration of a magnetic site as summarized in Table I in Ref. [S1]. We neglected terms that are higher order in λ .

We next consider a strong SOC case, where $\lambda \gg \Delta$ and the total angular momentum, a sum of spin momentum and angular momentum, is a constant of motion. The corresponding Eq. (2.45) is rewritten as

$$H_K = -\frac{1}{N} \sum_n \sum_{\mathbf{k}, \mathbf{k}'} \sum_{\nu, \nu'} e^{i(\mathbf{k}' - \mathbf{k}) \cdot \mathbf{R}_n} a_{\mathbf{k}\nu}^\dagger a_{\mathbf{k}'\nu'} \left[2(g_J - 1)(\mathbf{J}_n \cdot \mathbf{s}_{\nu\nu'}) \{F_0 + 2F_1(\boldsymbol{\kappa} \cdot \boldsymbol{\kappa}')\} + \frac{i}{2}(2 - g_J)F_2 \mathbf{J}_n \cdot (\boldsymbol{\kappa}' \times \boldsymbol{\kappa}) \right. \\ \left. + id_3 F_3 \left\{ (\mathbf{J}_n \cdot \mathbf{s}_{\nu\nu'}) (\mathbf{J}_n \cdot (\boldsymbol{\kappa}' \times \boldsymbol{\kappa})) + (\mathbf{J}_n \cdot (\boldsymbol{\kappa}' \times \boldsymbol{\kappa})) (\mathbf{J}_n \cdot \mathbf{s}_{\nu\nu'}) - \frac{2}{3} (\mathbf{J}_n \cdot \mathbf{J}_n) (\mathbf{s}_{\nu\nu'} \cdot (\boldsymbol{\kappa}' \times \boldsymbol{\kappa})) \right\} \right]. \quad (\text{S2})$$

Here, \mathbf{J}_n is a local total angular momentum at site \mathbf{R}_n , and g_J is the Landé g factor. d_3 is a dimensionless parameter of $\mathcal{O}(1/10)$ – $\mathcal{O}(1)$ depending on the electron configuration of a magnetic site. This parameter is defined in Eq. (2.48) in Ref. [S1]. We neglected terms which contain quadrupole moments because those terms do not contribute to the spin Hall (SH) effect.

In Eqs. (S1) and (S2), $F_{1,2,3}$ terms contain $\boldsymbol{\kappa}$ and $\boldsymbol{\kappa}'$, instead of \mathbf{k} and \mathbf{k}' . We rewrite these terms by replacing $\boldsymbol{\kappa}$ and $\boldsymbol{\kappa}'$ by \mathbf{k}/k_F and \mathbf{k}'/k_F , respectively. When k and k' are away from k_F , one has to consider higher order terms with respect to k and k' . These terms are expected to produce higher-order corrections with respect to temperature T in our results. However, such corrections are expected to be small because only $|\mathbf{k}| \sim k_F$ contributes in our analyses.

After this replacement, the correspondence between Eq. (1) in the main text and Eq. (S1) or (S2) is clearer. For a weak SOC case, $\mathbf{J}_n \Leftrightarrow \mathbf{S}_n$, $\mathcal{F}_0 \Leftrightarrow F_0$, $\mathcal{F}_1 \Leftrightarrow \frac{1}{k_F^2} F_1$, $\mathcal{F}_2 \Leftrightarrow \frac{1}{k_F^2} \Lambda_1 F_2$, and $\mathcal{F}_3 \Leftrightarrow \frac{2}{k_F^2} c_2 \Lambda_1 F_2$. For a strong SOC case, $\mathbf{J}_n \Leftrightarrow \mathbf{J}_n$, $\mathcal{F}_0 \Leftrightarrow (g_J - 1)F_0$, $\mathcal{F}_1 \Leftrightarrow \frac{1}{k_F^2} (g_J - 1)F_1$, $\mathcal{F}_2 \Leftrightarrow \frac{1}{k_F^2} (2 - g_J)F_2/2$, and $\mathcal{F}_3 \Leftrightarrow \frac{1}{k_F^2} d_3 F_3$. Thus, our model Eq. (1) unifies weak SOC and strong SOC cases.

S2. Side jump

The SH conductivity by the side-jump-type mechanism as diagrammatically shown in Fig. 2 is expressed in terms of the electron Green's function and the propagator of the spin fluctuation as

$$\begin{aligned} \sigma_{SH}^{side\ jump}(i\Omega_l) = & \frac{1}{i\Omega_l} \frac{2e^2}{m} \frac{T^2}{VN^3} \sum_{l,l'} \sum_{n,n'} \sum_{\mathbf{k},\mathbf{k}'} \left\{ \mathcal{F}_0 k_x^2 - 2\mathcal{F}_1 k_x^2 (k'_x)^2 \right\} \mathcal{F}_2 \\ & \times G_{\mathbf{k}}(i\varepsilon_l) G_{\mathbf{k}}(i\varepsilon_l + i\hbar\Omega_l) \{ G_{\mathbf{k}'}(i\varepsilon_{l'} + i\hbar\Omega_l) - G_{\mathbf{k}'}(i\varepsilon_{l'}) \} \\ & \times D_{\mathbf{k}'-\mathbf{k}}(i\varepsilon_{l'} - i\varepsilon_l) e^{i(\mathbf{k}'-\mathbf{k})\cdot(\mathbf{R}_n-\mathbf{R}_{n'})}, \end{aligned} \quad (\text{S3})$$

where, $G_{\mathbf{k}}(i\varepsilon_l) = \{i\varepsilon_l - \varepsilon_{\mathbf{k}} - \Sigma_{\mathbf{k}}(i\varepsilon_l)\}^{-1}$ is the electron Matsubara Green's function, with the fermionic Matsubara frequency $\varepsilon_l = (2l+1)\pi T$. Planck constant \hbar is included explicitly in front of the Matsubara frequency Ω_l .

After carrying out the Matsubara summation, and taking the limit of $i\Omega_l \rightarrow 0$, one obtains

$$\begin{aligned} \sigma_{SH}^{side\ jump} = & \frac{2e^2\hbar}{\pi mVN^3} \int d\varepsilon d\omega \sum_{n,n'} \sum_{\mathbf{k},\mathbf{k}'} \left\{ \mathcal{F}_0 k_x^2 - 2\mathcal{F}_1 k_x^2 (k'_x)^2 \right\} \mathcal{F}_2 B_{\mathbf{k}'-\mathbf{k}}(\omega) \{ b(\omega) + f(\varepsilon_{\mathbf{k}'}) \} \\ & \times \left[\partial_\varepsilon f(\varepsilon) |G_{\mathbf{k}}^R(\varepsilon)|^2 \Im \{ G_{\mathbf{k}'}^R(\varepsilon + \omega) \} + f(\varepsilon) \Im \{ G_{\mathbf{k}}^R(\varepsilon) G_{\mathbf{k}}^R(\varepsilon) \partial_\varepsilon G_{\mathbf{k}'}^R(\varepsilon + \omega) \} \right] e^{i(\mathbf{k}'-\mathbf{k})\cdot(\mathbf{R}_n-\mathbf{R}_{n'})}. \end{aligned} \quad (\text{S4})$$

$f(\varepsilon)$ and $b(\omega)$ are the Fermi distribution function and the Bose distribution function, respectively. $G_{\mathbf{k}}^{R,A}(\varepsilon) = G_{\mathbf{k}}(i\varepsilon_l \rightarrow \varepsilon \pm i\hbar/2\tau_c)$ are the retarded and advanced Green's function, respectively. Here, the self-energy is assumed to be independent of ε , and τ_c is the carrier lifetime. $B_{\mathbf{q}}(\omega)$ is the spectral function of the J propagator given by $B_{\mathbf{q}}(\omega) = -\frac{1}{\pi} \Im D_{\mathbf{q}}(i\omega_l \rightarrow \omega + i0^+) = \frac{1}{\pi} \frac{\omega/\Gamma_q}{(\delta + Aq^2)^2 + (\omega/\Gamma_q)^2}$.

The first term in the square bracket of Eq. (S4) is proportional to $\partial_\varepsilon f(\varepsilon) \approx -\delta(\varepsilon)$, the so-called Fermi surface term, while the second term is proportional to $f(\varepsilon)$, the so-called Fermi sea term. In principle, two terms contribute, but it can be shown that the contribution from the second term, the Fermi sea term, is small. Thus, we focus on the first contribution.

We use the following approximations considering the small self-energy $\Sigma_{\mathbf{k}}(\varepsilon) = i\hbar/2\tau_c$: $|G_{\mathbf{k}}^R(\varepsilon)|^2 \approx (2\pi\tau_c/\hbar)\delta(\varepsilon - \varepsilon_{\mathbf{k}})$ and $\Im G_{\mathbf{k}}^R(\varepsilon) \approx -\pi\delta(\varepsilon - \varepsilon_{\mathbf{k}})$. Performing the ε and ω integrals in Eq. (S4), one obtains

$$\sigma_{SH}^{side\ jump} \approx \frac{2e^2\pi\tau_c}{mVN^3} \sum_{n,n'} \sum_{\mathbf{k},\mathbf{k}'} \delta(\varepsilon_{\mathbf{k}}) \left\{ \mathcal{F}_0 k_x^2 - 2\mathcal{F}_1 k_x^2 (k'_x)^2 \right\} \mathcal{F}_2 B_{\mathbf{k}'-\mathbf{k}}(\varepsilon_{\mathbf{k}'}) \{ b(\varepsilon_{\mathbf{k}'}) + f(\varepsilon_{\mathbf{k}'}) \} e^{i(\mathbf{k}'-\mathbf{k})\cdot(\mathbf{R}_n-\mathbf{R}_{n'})}. \quad (\text{S5})$$

Noticing that $B_{\mathbf{k}'-\mathbf{k}}$ is dominated by small $|\mathbf{k}' - \mathbf{k}|$ regions, we replace \mathbf{k}' by $\mathbf{k} + \mathbf{q}$ and $e^{i\mathbf{q}\cdot(\mathbf{R}_n-\mathbf{R}_{n'})}$ by 1. Then, $\varepsilon_{\mathbf{k}'}$ is approximated as $\varepsilon_{\mathbf{k}'} = \frac{\hbar^2}{2m} |\mathbf{k} + \mathbf{q}|^2 - \mu \approx \varepsilon_{\mathbf{k}} - \mu + \hbar\mathbf{v}_F \cdot \mathbf{q}$ near the Fermi level, with \mathbf{v}_F being the Fermi velocity parallel to \mathbf{k} . This leads to

$$\sigma_{SH}^{side\ jump} \approx \frac{2e^2\pi\tau_c}{mVN} n_m^2 \sum_{\mathbf{k},\mathbf{q}} \delta(\varepsilon_{\mathbf{k}}) \left\{ \mathcal{F}_0 k_x^2 - 2\mathcal{F}_1 k_x^2 (k_x + q_x)^2 \right\} \mathcal{F}_2 B_{\mathbf{q}}(\hbar\mathbf{v}_F \cdot \mathbf{q}) \{ b(\hbar\mathbf{v}_F \cdot \mathbf{q}) + f(\hbar\mathbf{v}_F \cdot \mathbf{q}) \}. \quad (\text{S6})$$

Here, $n_m = N_m/N$ is the concentration of local moments. By neglecting small corrections coming from q_x^2 , the \mathbf{q} integral is summarized into the following function,

$$I(T, \delta) \equiv \frac{\pi}{N} \sum_{\mathbf{q}} B_{\mathbf{q}}(\hbar\mathbf{v}_F \cdot \mathbf{q}) \{ b(\hbar\mathbf{v}_F \cdot \mathbf{q}) + f(\hbar\mathbf{v}_F \cdot \mathbf{q}) \}. \quad (\text{S7})$$

Combining Eqs. (S6) and (S7), one arrives at Eq. (4).

S3. Skew scattering

Using Matsubara Green's functions for conduction electrons and the spin fluctuation, the SH conductivity due to the skew-type scattering is expressed as

$$\begin{aligned}
\sigma_{SH}^{skew\,scat.}(i\Omega_l) = & \frac{1}{i\Omega_l} \frac{e^2 \hbar^2}{m^2} \frac{T^3}{VN^5} \sum_{l,l',l''} \sum_{n,n',n''} \sum_{\mathbf{k},\mathbf{k}',\mathbf{k}''} \\
& \times G_{\mathbf{k}}(i\varepsilon_l) G_{\mathbf{k}}(i\varepsilon_l + i\hbar\Omega_l) G_{\mathbf{k}'}(i\varepsilon_{l'}) G_{\mathbf{k}'}(i\varepsilon_{l'} + i\hbar\Omega_l) \{G_{\mathbf{k}''}(i\varepsilon_{l''} + i\hbar\Omega_l) - G_{\mathbf{k}''}(i\varepsilon_{l''})\} \\
& \times \left\{ -D_{\mathbf{k}-\mathbf{k}''}(i\varepsilon_l - i\varepsilon_{l''}) D_{\mathbf{k}'-\mathbf{k}''}(i\varepsilon_{l'} - i\varepsilon_{l''}) \mathcal{F}_3 k_x^2 k_y'^2 (\mathcal{F}_0 + \mathcal{F}_1 \mathbf{k} \cdot \mathbf{k}'') (\mathcal{F}_0 + \mathcal{F}_1 \mathbf{k}' \cdot \mathbf{k}'') \right. \\
& \times e^{i(\mathbf{k}-\mathbf{k}'') \cdot (\mathbf{R}_{n'} - \mathbf{R}_n) + i(\mathbf{k}' - \mathbf{k}'') \cdot (\mathbf{R}_n - \mathbf{R}_{n''})} \\
& + 2D_{\mathbf{k}-\mathbf{k}'}(i\varepsilon_l - i\varepsilon_{l'}) D_{\mathbf{k}''-\mathbf{k}'}(i\varepsilon_{l''} - i\varepsilon_{l'}) \mathcal{F}_3 k_x^2 k_y'' k_y' (\mathcal{F}_0 + \mathcal{F}_1 \mathbf{k} \cdot \mathbf{k}') (\mathcal{F}_0 + \mathcal{F}_1 \mathbf{k}' \cdot \mathbf{k}'') \\
& \left. \times e^{i(\mathbf{k}-\mathbf{k}') \cdot (\mathbf{R}_{n'} - \mathbf{R}_n) + i(\mathbf{k}'' - \mathbf{k}') \cdot (\mathbf{R}_n - \mathbf{R}_{n''})} \right\}. \tag{S8}
\end{aligned}$$

Here, the last term in Eq. (1) is not considered because this term is proportional to $(\mathbf{J}_n \cdot \mathbf{J}_n) \approx const..$ The Matsubara summation can be carried out similarly as in the side-jump mechanism, leading to

$$\begin{aligned}
\sigma_{SH}^{skew\,scat.} = & \frac{e^2 \hbar^3}{\pi m^2 V N^5} \int d\varepsilon d\omega d\omega' \sum_{n,n',n''} \sum_{\mathbf{k},\mathbf{k}',\mathbf{k}''} \\
& \times \left[\mathcal{F}_3 k_x^2 k_y'^2 (\mathcal{F}_0 + \mathcal{F}_1 \mathbf{k} \cdot \mathbf{k}'') (\mathcal{F}_0 + \mathcal{F}_1 \mathbf{k}' \cdot \mathbf{k}'') B_{\mathbf{k}-\mathbf{k}''}(\omega) \{b(\omega) + f(\varepsilon_{\mathbf{k}})\} B_{\mathbf{k}'-\mathbf{k}''}(\omega') \{b(\omega') + f(\varepsilon_{\mathbf{k}'})\} \right. \\
& \times \left\{ \partial_\varepsilon f(\varepsilon) |G_{\mathbf{k}}^R(\varepsilon + \omega)|^2 |G_{\mathbf{k}'}^R(\varepsilon + \omega')|^2 \Im \{G_{\mathbf{k}''}^R(\varepsilon)\} + f(\varepsilon) \Im \{ (G_{\mathbf{k}}^R(\varepsilon + \omega) G_{\mathbf{k}'}^R(\varepsilon + \omega'))^2 \partial_\varepsilon G_{\mathbf{k}''}^R(\varepsilon) \} \right\} \\
& \times e^{i(\mathbf{k}-\mathbf{k}'') \cdot (\mathbf{R}_{n'} - \mathbf{R}_n) + i(\mathbf{k}' - \mathbf{k}'') \cdot (\mathbf{R}_n - \mathbf{R}_{n''})} \\
& - 2\mathcal{F}_3 k_x^2 k_y'' k_y' (\mathcal{F}_0 + \mathcal{F}_1 \mathbf{k} \cdot \mathbf{k}') (\mathcal{F}_0 + \mathcal{F}_1 \mathbf{k}' \cdot \mathbf{k}'') B_{\mathbf{k}-\mathbf{k}'}(\omega) \{b(\omega) + f(\varepsilon_{\mathbf{k}})\} B_{\mathbf{k}''-\mathbf{k}'}(\omega') \{b(\omega') + f(\varepsilon_{\mathbf{k}'})\} \\
& \times \left\{ \partial_\varepsilon f(\varepsilon) |G_{\mathbf{k}}^R(\varepsilon + \omega)|^2 |G_{\mathbf{k}'}^R(\varepsilon)|^2 \Im \{G_{\mathbf{k}''}^R(\varepsilon + \omega')\} + f(\varepsilon) \Im \{ (G_{\mathbf{k}}^R(\varepsilon + \omega) G_{\mathbf{k}'}^R(\varepsilon))^2 \partial_\varepsilon G_{\mathbf{k}''}^R(\varepsilon + \omega') \} \right\} \\
& \left. \times e^{i(\mathbf{k}-\mathbf{k}') \cdot (\mathbf{R}_{n'} - \mathbf{R}_n) + i(\mathbf{k}'' - \mathbf{k}') \cdot (\mathbf{R}_n - \mathbf{R}_{n''})} \right]. \tag{S9}
\end{aligned}$$

Again, we focus on the Fermi surface terms which are proportional to $\partial_\varepsilon f(\varepsilon)$. Carrying out ε , ω and ω' integrals, one obtains

$$\begin{aligned}
\sigma_{SH}^{skew\,scat.} \approx & \frac{4e^2 \hbar \pi^2 \tau_c^2}{m^2 V N^5} \sum_{n,n',n''} \sum_{\mathbf{k},\mathbf{k}',\mathbf{k}''} \delta(\varepsilon_{\mathbf{k}''}) B_{\mathbf{k}-\mathbf{k}''}(\varepsilon_{\mathbf{k}}) \{b(\varepsilon_{\mathbf{k}}) + f(\varepsilon_{\mathbf{k}})\} B_{\mathbf{k}'-\mathbf{k}''}(\varepsilon_{\mathbf{k}'}) \{b(\varepsilon_{\mathbf{k}'}) + f(\varepsilon_{\mathbf{k}'})\} \\
& \times \{ -\mathcal{F}_3 k_x^2 k_y'^2 (\mathcal{F}_0 + \mathcal{F}_1 \mathbf{k} \cdot \mathbf{k}'') (\mathcal{F}_0 + \mathcal{F}_1 \mathbf{k}' \cdot \mathbf{k}'') + 2\mathcal{F}_3 k_x^2 k_y'' k_y' (\mathcal{F}_0 + \mathcal{F}_1 \mathbf{k} \cdot \mathbf{k}'') (\mathcal{F}_0 + \mathcal{F}_1 \mathbf{k}' \cdot \mathbf{k}'') \} \\
& \times e^{i(\mathbf{k}-\mathbf{k}'') \cdot (\mathbf{R}_{n'} - \mathbf{R}_n) + i(\mathbf{k}' - \mathbf{k}'') \cdot (\mathbf{R}_n - \mathbf{R}_{n''})}. \tag{S10}
\end{aligned}$$

As in the side-jump case, main contributions are from small $|\mathbf{k} - \mathbf{k}''|$ and small $|\mathbf{k}' - \mathbf{k}''|$ regions. Thus, expanding \mathbf{k} and \mathbf{k}' from \mathbf{k}'' as $\mathbf{k} = \mathbf{k}'' + \mathbf{q}$ and $\mathbf{k}' = \mathbf{k}'' + \mathbf{q}'$ approximating $e^{i(\mathbf{k}-\mathbf{k}'') \cdot (\mathbf{R}_{n'} - \mathbf{R}_n) + i(\mathbf{k}' - \mathbf{k}'') \cdot (\mathbf{R}_n - \mathbf{R}_{n''})}$ by 1, and replacing \mathbf{q} integrals by $I(T, \delta)$ defined in Eq. (S7), one arrives at Eq. (5).

S4. Detail of $I(T, \delta)$

Focusing on low temperature regimes where the linear approximation $\varepsilon_{\mathbf{k}'} \approx \hbar \mathbf{v}_F \cdot \mathbf{q}$ is justified, we further approximate $b(\hbar \mathbf{v}_F \cdot \mathbf{q}) + f(\hbar \mathbf{v}_F \cdot \mathbf{q}) \approx T/\hbar \mathbf{v}_F \cdot \mathbf{q}$ to arrive at

$$I(T, \delta) \approx \frac{1}{N} \sum_{\mathbf{q}} \frac{T/\Gamma_q}{(\delta + Aq^2)^2 + (\hbar \mathbf{v}_F \cdot \mathbf{q}/\Gamma_q)^2}. \tag{S11}$$

Considering a three dimensional system, the \mathbf{q} integral is evaluated as

$$\begin{aligned} I(T, \delta) &\approx \frac{a^3}{(2\pi)^3} \int_0^{T/\hbar v_F} dq \int_0^\pi d\theta \frac{2\pi q^2 T \sin \theta / \Gamma_q}{(\delta + Aq^2)^2 + (\hbar v_F q \cos \theta / \Gamma_q)^2} \\ &= \frac{a^3}{(2\pi)^2} \int_0^{T/\hbar v_F} dq \frac{T}{\hbar v_F} \frac{2q}{\delta + Aq^2} \arctan \frac{\hbar v_F q / \Gamma_q}{\delta + Aq^2}, \end{aligned} \quad (\text{S12})$$

with a being the lattice constant.

Now, we consider limiting cases, where the analytic form of $I(T, \delta)$ is available.

(1) *Clean metals at low temperatures where $\delta + A(T/\hbar v_F)^2 \ll \hbar v_F / \Gamma$.* In this case, \arctan is approximated as $\pi/2$, leading to

$$I(T, \delta) \approx \frac{a^3}{(2\pi)^2} \int_0^{T/\hbar v_F} dq \frac{T}{A\hbar v_F} \frac{\pi q}{\delta + Aq^2} = \frac{1}{8\pi} \frac{a^3 T}{A\hbar v_F} \ln \left[1 + \frac{A}{\delta} \left(\frac{T}{\hbar v_F} \right)^2 \right] \approx \frac{1}{8\pi\delta} \left(\frac{aT}{\hbar v_F} \right)^3. \quad (\text{S13})$$

Near the FM critical point, δ is scaled as $\delta \propto T^{4/3}$ [S2]. Therefore, $I(T, \delta)$ is expected to be scaled as $T^{5/3}$

(2) *Clean metals at high temperatures with $\delta + A(T/\hbar v_F)^2 \gg \hbar v_F / \Gamma$.* In this case, we expand the argument of \arctan to get

$$I(T, \delta) \approx \frac{a^3}{(2\pi)^2} \int_0^{T/\hbar v_F} dq \frac{T}{\hbar v_F} \frac{2q\hbar v_F / \Gamma}{(\delta + Aq^2)^2} = \frac{1}{(2\pi)^2} \frac{\hbar v_F}{\Gamma} \left(\frac{aT}{\hbar v_F} \right)^3 \frac{1}{\delta \{ \delta + A(T/\hbar v_F)^2 \}}. \quad (\text{S14})$$

At such high temperatures, δ is linearly proportional to T [S2, S3]. Therefore, $I(T, \delta)$ is expected to be proportional to T .

(3) *Dirty metals at low temperatures with $T \ll \Gamma q_c \delta$.* In this case, we take $\Gamma_q = \Gamma_{q_c}$ and expand the argument of \arctan to get

$$\begin{aligned} I(T, \delta) &\approx \frac{a^3}{(2\pi)^2} \int_0^{T/\hbar v_F} dq \frac{T}{\hbar v_F} \frac{2q^2 \hbar v_F / \Gamma_{q_c}}{(\delta + Aq^2)^2} = \frac{a^3}{(2\pi)^2} \frac{\hbar v_F}{\Gamma_{q_c}} \frac{T}{\hbar v_F} \left[\frac{1}{A\sqrt{A\delta}} \arctan \sqrt{\frac{A}{\delta}} q - \frac{q}{A(\delta + Aq^2)} \right]_0^{T/\hbar v_F} \\ &\approx \frac{1}{(2\pi)^2} \frac{\hbar v_F}{a\Gamma_{q_c}} \left(\frac{aT}{\hbar v_F} \right)^4 \frac{1}{\delta \{ \delta + A(T/\hbar v_F)^2 \}}. \end{aligned} \quad (\text{S15})$$

Since the damping Γ_q is independent of q in this temperature regime, δ is scaled as $\delta \propto T^{3/2}$ [S4]. Therefore, $I(T, \delta)$ is expected to be proportional to T .

(4) *Dirty metals at moderately high temperatures with $T > \Gamma_{q_c} \delta$.* In this case, we expand the argument of \arctan and separate the q integral into two regions, $q \leq q_c$ and $q \geq q_c$. This leads to

$$\begin{aligned} I(T, \delta) &\approx \frac{a^3}{(2\pi)^2} \frac{T}{\hbar v_F} \left\{ \int_0^{q_c} dq \frac{2q^2 \hbar v_F / \Gamma_{q_c}}{(\delta + Aq^2)^2} + \int_{q_c}^{T/\hbar v_F} dq \frac{2q \hbar v_F / \Gamma}{(\delta + Aq^2)^2} \right\} \\ &= \frac{a^3}{(2\pi)^2} \frac{T}{\hbar v_F} \left\{ \frac{\hbar v_F}{\Gamma_{q_c}} \left[\frac{1}{A\sqrt{A\delta}} \arctan \sqrt{\frac{A}{\delta}} q - \frac{q}{A(\delta + Aq^2)} \right]_0^{q_c} - \frac{\hbar v_F}{\Gamma} \left[\frac{1}{A\{ \delta + Aq^2 \}} \right]_{q_c}^{T/\hbar v_F} \right\} \\ &= \frac{a^3}{(2\pi)^2} \frac{T}{\hbar v_F} \left\{ \frac{\hbar v_F}{\Gamma_{q_c}} \left[\frac{1}{A\sqrt{A\delta}} \arctan \sqrt{\frac{A}{\delta}} q_c - \frac{q_c}{A(\delta + Aq_c^2)} \right] - \frac{\hbar v_F}{\Gamma} \left[\frac{1}{A\{ \delta + A(T/\hbar v_F)^2 \}} - \frac{1}{A\{ \delta + Aq_c^2 \}} \right] \right\} \\ &\approx \frac{1}{(2\pi)^2} \frac{\hbar v_F}{\Gamma} \left(\frac{aT}{\hbar v_F} \right)^3 \frac{1}{\delta \{ \delta + A(T/\hbar v_F)^2 \}} \end{aligned} \quad (\text{S16})$$

The final form is the same as Eq. (S14). In this temperature regime, δ is proportional to T [S2, S3]. Therefore $I(T, \delta)$ is also proportional to T .

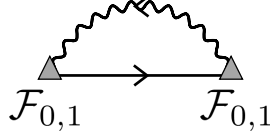


FIG. S1: Diagrammatic representation for the electron self-energy.

S5. Carrier lifetime by the spin fluctuation

Here, we consider the electron self-energy $\Sigma_{\mathbf{k}}(i\varepsilon_l)$ due to the coupling with the spin fluctuation. The lowest order self-energy is given by (see Fig. S1 for the diagrammatic representation)

$$\Sigma_{\mathbf{k}}(i\varepsilon_l) = \frac{T}{N^3} \sum_{n,n'} \sum_{\mathbf{q}, i\omega_{l'}} e^{i(\mathbf{k}+\mathbf{q}) \cdot (\mathbf{R}_n - \mathbf{R}_{n'})} \left\{ \mathcal{F}_0 + 2\mathcal{F}_1(k^2 + \mathbf{k} \cdot \mathbf{q}) \right\}^2 G_{\mathbf{k}+\mathbf{q}}(i\varepsilon_l + i\omega_{l'}) D_{\mathbf{q}}(i\omega_{l'}). \quad (\text{S17})$$

After carrying out the Matsubara summation and the analytic continuation $i\varepsilon_l \rightarrow \varepsilon + i\eta$ with $i\eta$ being a small imaginary number, the imaginary part of the self-energy becomes

$$\Im \Sigma_{\mathbf{k}}(\varepsilon) \approx -\frac{\pi}{N^3} \sum_{\mathbf{q}} \int d\omega e^{i(\mathbf{k}+\mathbf{q}) \cdot (\mathbf{R}_n - \mathbf{R}_{n'})} \left\{ \mathcal{F}_0 + 2\mathcal{F}_1(k^2 + \mathbf{k} \cdot \mathbf{q}) \right\}^2 B_{\mathbf{q}}(\omega) \{b(\omega) + f(\omega + \varepsilon)\} \delta(\varepsilon + \omega - \varepsilon_{\mathbf{k}+\mathbf{q}}). \quad (\text{S18})$$

As in the SH conductivity, we focus on the low-energy part $\varepsilon = 0$, approximate $\varepsilon_{\mathbf{k}+\mathbf{q}} \approx \hbar \mathbf{v}_F \cdot \mathbf{q}$ and $e^{i(\mathbf{k}+\mathbf{q}) \cdot (\mathbf{R}_n - \mathbf{R}_{n'})} \approx 1$. This leads to

$$\Im \Sigma_{\mathbf{k}}(0) \approx -\frac{\pi}{N} n_m^2 \sum_{\mathbf{q}} \left\{ \mathcal{F}_0 + 2\mathcal{F}_1(k^2 + \mathbf{k} \cdot \mathbf{q}) \right\}^2 B_{\mathbf{q}}(\hbar \mathbf{v}_F \cdot \mathbf{q}) \{b(\hbar \mathbf{v}_F \cdot \mathbf{q}) + f(\hbar \mathbf{v}_F \cdot \mathbf{q})\}. \quad (\text{S19})$$

Neglecting the small contribution from $\mathbf{k} \cdot \mathbf{q}$, one obtains for $k = k_F$

$$\Im \Sigma_{k_F}(0) \approx -n_m^2 (F_0 + 2F_1 k_F^2)^2 I(T, \delta) = -\hbar/2\tau_{sf}. \quad (\text{S20})$$

S6. Maximum $\sigma_{SH}^{side\ jump}$ and $\sigma_{SH}^{skew\ scat.}$

Here, we consider $\tau_c I(T, \delta)$ at low temperatures in the clean limit. Parameterizing the carrier lifetime by the spin fluctuation as $\tau_{sf}^{-1} = \tau_{sf,0}^{-1} (T/T_{sf})^{5/3}$ and $I(T, \delta) = \alpha (T/T_{sf})^{5/3}$, where $T_{sf} = \hbar v_F/a$, we differentiate $\tau_c I(T, \delta)$ with $\tau_c^{-1} = \tau_{sf}^{-1} + \tau_{dis}^{-1} + \tau_{ee}^{-1} + \tau_{ep}^{-1}$ with respect to T as

$$\begin{aligned} \frac{d\tau_c I(T, \delta)}{dT} &= \alpha \tau_c^2 \left[\frac{5}{3T_{sf}} \left(\frac{T}{T_{sf}} \right)^{2/3} \tau_c^{-1} - \left(\frac{T}{T_{sf}} \right)^{5/3} \left\{ \tau_{sf,0}^{-1} \frac{5}{3T_{sf}} \left(\frac{T}{T_{sf}} \right)^{2/3} + \tau_{ee,0}^{-1} \frac{2}{T_F} \left(\frac{T}{T_F} \right) + \tau_{ep,0}^{-1} \frac{5}{T_D} \left(\frac{T}{T_D} \right)^4 \right\} \right] \\ &= \frac{5\alpha\tau_c^2}{3T_{sf}} \left(\frac{T}{T_{sf}} \right)^{2/3} \left[\tau_{dis}^{-1} - \frac{1}{5} \tau_{ee,0}^{-1} \left(\frac{T}{T_F} \right)^2 - 2\tau_{ep,0}^{-1} \left(\frac{T}{T_D} \right)^5 \right] = 0. \end{aligned} \quad (\text{S21})$$

An approximate solution for this equation is $T_{max} = T_F (5\tau_{ee,0}/\tau_{dis})^{1/2}$ for $T_F \ll T_D$ or $T_{max} = T_D (\tau_{ep,0}/2\tau_{dis})^{1/5}$ for $T_F \gg T_D$.

At this temperature, $\tau_c I(T, \delta)$ becomes

$$\tau_c I(T, \delta) = \alpha \left(\frac{T_F}{T_{sf}} \right)^{5/3} \left(\frac{5\tau_{ee,0}}{\tau_{dis}} \right)^{5/6} \left\{ 6\tau_{dis}^{-1} + \tau_{sf,0}^{-1} \left(\frac{T_F}{T_{sf}} \right)^{5/3} \left(\frac{5\tau_{ee,0}}{\tau_{dis}} \right)^{5/6} \right\}^{-1} \quad (\text{S22})$$

for $T_F \ll T_D$, or

$$\tau_c I(T, \delta) = \alpha \left(\frac{T_D}{T_{sf}} \right)^{5/3} \left(\frac{\tau_{ep,0}}{2\tau_{dis}} \right)^{1/3} \left\{ \frac{3}{2} \tau_{dis}^{-1} + \tau_{sf,0}^{-1} \left(\frac{T_D}{T_{sf}} \right)^{5/3} \left(\frac{5\tau_{ep,0}}{\tau_{dis}} \right)^{1/3} \right\}^{-1} \quad (\text{S23})$$

for $T_F \gg T_D$.

When $\tau_{dis}^{-1} \ll \tau_{sf,0}^{-1}$, $\tau_c I(T, \delta) \approx \alpha \tau_{sf,0}$. This leads to Eq. (7).

Similar analysis can be done for the dirty limit. The expression for T_{max} is the same as the clean limit. However, the leading term of $\sigma_{SH,max}^{side\ jump}$ explicitly depends on both τ_{dis} and $\tau_{ee,0}$ or $\tau_{ep,0}$.

Skew scattering contribution $\sigma_{SH}^{skew\ scat.}$ is proportional to $\tau_c^2 F^2(T, \delta)$. Therefore, $\sigma_{SH}^{skew\ scat.}$ is expected to be maximized to be $\sigma_{SH,max}^{skew\ scat.}$ in Eq. (8) at the same temperature T_{max} as $\sigma_{SH}^{side\ jump}$.

[S1] J. Kondo, Prog. Theor. Phys. **27**, 772 (1962).

[S2] T. Moriya, *Spin Fluctuations in Itinerant Electron Magnetism*, Solid-State Sciences **56** (Springer-Verlag, Berlin, 1985).

[S3] K. Ueda and T. Moriya, J. Phys. Soc. Jpn. **39**, 605 (1975).

[S4] N. Nagaosa, *Quantum Field Theory in Strongly Correlated Electron Systems* (Springer-Verlag, Berlin, 1999).